Microchimica Acta
https://doi.org/10.1007/s00604-018-3225-4

ORIGINAL PAPER

Colorimetric and fluorometric dual-channel detection of α-fetoprotein based on the use of ZnS-CdTe hierarchical porous nanospheres

Dong Zhu[1,2] · Yue Hu[1] · Xiao-Jing Zhang[1] · Xiao-Tong Yang[1] · Ying-Ying Tang[1]

Received: 17 October 2018 / Accepted: 29 December 2018

Abstract

An immunoassay is described for either colorimetric and fluorometric determination of the cancer biomarker α-fetoprotein (AFP). It is making use of ZnS nanospheres modified with CdTe quantum dots (QDs). These display strong fluorescence due to the enrichment of the QDs onto the porous ZnS nanospheres. In this assay, the release of millions of zinc(II) ions can be triggered to form a purple complex (with an absorption maximum at 571 nm) on addition of the reagent 2-(5-nitro-2-pyridylazo)-5-(N-propyl-N-sulfopropylamino) phenol. This results in a sensitive colorimetric immunoassay which can also be used as a visual test. It represents an enzyme-free alternative to the commonly used ELISAs. It also can be evaluated by fluorometry (with excitation/emission maxima at 400/645 nm). The detection limits are 10 pg·mL^{-1} for fluorometry and 7 pg·mL^{-1} for colorimetry. This sensitivity is better by one order of magnitude than that of the commercial ELISA. The dual detection feature provides good complementarity and reduces the risk of false-positive or false-negative results.

Keywords Optical biosensor · Enzyme-free bioassay · Zinc-based amplification · Dual functional detection · Biomarker · Immunoassay · Fluorescent nanomaterials · Chromogenic complex · Nitro-PAPS · Sandwich assay

Introduction

Simple and affordable biosensors of disease biomarker are extremely desired for public health especially at resource constrained areas or countries [1]. Enzyme-linked immunosorbent assay (ELISA) is a dominating gold standard [2]. However, this colorimetric bioassay gives only a relatively low sensitivity compared to other approaches especially those based on electrochemistry [3, 4] or fluorescence [5, 6].

In a typical colorimetric bioassay such as ELISA, the color signal is generated by the conversion of the enzymes conjugated with antibodies which can capture target, into a coloured substance. Accordingly, the enhanced sensitivity was partly accomplished by loading as many enzyme molecules as possible on certain carriers such as nanoparticles and polymers [7, 8]. The plasmonic ELISA by controlling the growth of gold nanoparticles and generating coloured signals also obtain the sensitive colorimetric detection even with the bare eye [9–14]. Despite these efforts, the detection sensitivity for the colorimetric bioassay is ultimately limited by the catalytic efficiency and the loading quantity of enzymes.

Quantum dots (QDs) as luminescence and electrochemiluminescence (ECL) labels for biosensors have attracted special attention owing to their advantages with broad excitation spectra, narrow emissions and feasibility for surface modification [15–20]. However, the requirement of complicated multiple-step approaches and highly delicate experimental skills restricts its further application. Moreover, the relatively few biomolecules conjugated onto the QDs owing to small surface area of the solid QDs also hampers the improvement of the bioassay sensitivity.

Herein, we describe an enzyme-free amplification approach to break the intrinsic limit of sensitivity for the colorimetric bioassay based on the release of Zn from the ZnS-CdTe nanospheres, achieving large-enhanced detection sensitivity. The biosensor that features a dual-mode detection combing colorimetry with the bare eye and fluorometry for

Electronic supplementary material The online version of this article (https://doi.org/10.1007/s00604-018-3225-4) contains supplementary material, which is available to authorized users.

✉ Dong Zhu
dongzhu@njucm.edu.cn

[1] Jiangsu Key Laboratory for Pharmacology and Safety Evaluation of Chinese Materia Medica, School of Pharmacy, Nanjing University of Chinese Medicine, Nanjing, Jiangsu 210023, People's Republic of China

[2] Jiangsu Key Laboratory for Functional Substance of Chinese Medicine, Nanjing, China

Published online: 23 January 2019

the alpha-fetoprotein (AFP, a typical tumor biomarker), by only using fluorescent ZnS-CdTe porous nanospheres based on in-situ synthesis of CdTe quantum dots as shown in Fig. 1. Moreover, this dual mode detection accomplished by only one immunoreaction features good complementarity and can reduce largely possible risk of false positive or negative result with single-mode detection in the ELISA or other bioassays [21–25].

As shown in Fig. 1, the detection sensitivity can be enhanced through two rounds of amplification. In the first round, detection antibodies (denoted as Ab2) were conjugated with ZnS-CdTe nanospheres, and sensitive fluorometry detection can be achieved directly by increasing the ZnS-CdTe loading per sandwich immunoreaction. Besides, ZnS-CdTe nanospheres were dissolved in the solution of nitric acid to produce millions of zinc ions, which can form a distinct purple complex when the reagent of 2-(5-nitro-2-pyridylazo)-5-(N-propyl-N-sulfopropylamino) phenol disodium salt dihydrate (Nitro-PAPS) was given to develop a colorimetry which can even be observed only with the bare eye. To the best of my knowledge, the colorimetric biosensor dependent upon the release of Zn from nanospheres have not been reported. In the second round, the large surface of porous structure ZnS nanospheres is able to load many hundreds of Ab2 (6600 Ab2 per ZnS-CdTe in this study). This Ab2/ZnS-CdTe format can specifically recognize the target analyte that was bond by the capture antibody (denoted as Ab1). Very small amounts of the targets can thus be detected because of the high density of Ab2. Moreover, plenty of CdTe QDs in-situ synthesized onto the surface of the ZnS nanospheres (360 QDs per ZnS nanosphere) brings about great enhancement of the fluoro-biosensor sensitivity.

Experimental section

Chemicals and materials

Cysteamine, gum arabic (GA), DL-dithiothreitol and mercaptosuccinic acid were purchased from Aladdin-reagent Chemical Reagent (Shanghai) Co., Ltd. (http://www.aladdin-e.com). $ZnAc_2{\cdot}2H_2O$, thioacetamide (TAA), cadmium chloride, sodium dodecyl sulfate (SDS) and sodium tellurite were purchased from Nanjing Chemical Reagent Co., Ltd. (http://www.nj-reagent.com). 1-ethyl-3-(3-dimethylaminopropyl) carbodiimide hydrochloride (EDC), N-hydroxysuccinimide (NHS) were obtained from Shanghai Aladdin-reagent Chemical Reagent Co., Ltd. 2-(5-nitro-2-pyridylazo)-5-(N-propyl-N-sulfopropylamino) phenol disodium salt dihydrate (Nitro-PAPS) was purchased by Shanghai dumabio Co.Ltd. (http://www.dumabio.com). BSA (bovine serum albumin) was purchased from Sigma-Aldrich (https://www.sigmaaldrich.com). 96-well polystyrene plates were purchased from Corning Incorporated (http://www.corning.com). The anti-AFP rabbit polyclonal antibody (Ab1) and anti-AFP mouse monoclonal antibody (Ab2) were obtained by Sangon Biotech (Shanghai) Co., Ltd. (https://www.sangon.com/). Bicinchoninic acid (BCA) protein assay

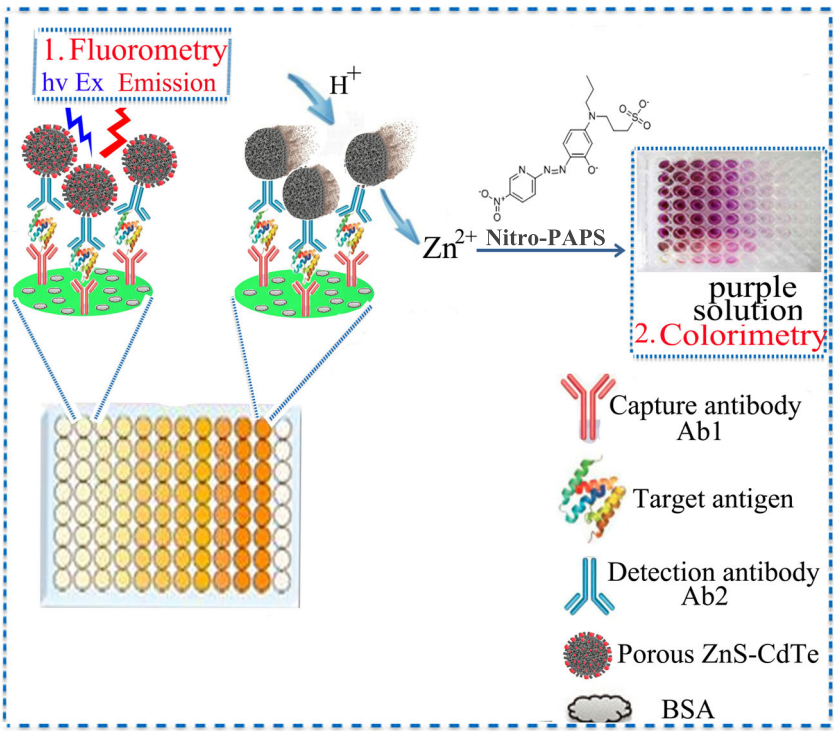

Fig. 1 Biosensor that features a dual-mode detection of biomarkers combing colorimetry with the bare eye and fluorometry by only using CdTe QDs embedded ZnS porous nanospheres (ZnS-CdTe) (CdTe QDs in-situ synthesized onto the surface of porous ZnS nanospheres) as labels

kit was obtained from Sangon Biotech (Shanghai) Co., Ltd. (www.beyotime.com). Ultrapure water (18 MΩ·cm) from a Millipore system was used to prepare solutions throughout the assay. All chemicals were analytic reagents and used as received without any purification.

Apparatus and characterization

Transmission electron microscopy (TEM) characterization was carried out on a Tecnai G2 F20 S-Twin electron microscope (FEI Company, Hillsboro, OR, USA). Multiple functional Microwell plates (Spark 10 M, Tecan) were used to measurement of fluorescence and Uv-vis mode. The UV-vis absorbance measurement was performed with a UV 2401 spectrophotometer (Shimadzu Scientific, Japan). The surface measurement was performed by nitrogen sorption isotherms at 77 K with a micromeritics ASAP2020 instrument (Micromeritics, Norcross, GA, USA). The surface areas were calculated by the Brunauer-Emmett–Teller (BET) method, and the pore size distributions were calculated by the Barrett-Joyner-Halenda (BJH) method. Inductively coupled plasma atomic emission spectroscopy (ICP-AES) was performed on a Perkin-Elmer Optima 3000 DV after dissolving the ZnS-CdTe nanospheres in 5% hydrochloric acid.

CdTe quantum dots (QDs) in-situ synthesized onto the surface of ZnS porous nanospheres (ZnS-CdTe)

Firstly, the porous ZnS nanosphere was synthesized via previous method [20] with slight modifications (See Electronic Supporting Material). The prepared ZnS nanospheres were functionalized with DL-dithiothreitol. Briefly, 100 mg of ZnS nanospheres were dispersed in 50 mL of dehydrated ethanol and then purged slowly with dry nitrogen for 60 min to exclude the oxygen in the ethanol. Then, 2.5 mmol of DL-dithiothreitol was added into the above solution, and the solution was gently stirred for 24 h in a sealed vessel. The prepared thiol-modified ZnS nanospheres were centrifuged and washed with ethanol three times to remove the unreacted dithiothreitol. Subsequently, thiol-capped ZnS nanospheres (50 mg) solution mixed with cadmium chloride ($CdCl_2$, 0.04 mol·L^{-1}, 4 mL) and trisodium citrate dihydrate (200 mg) was diluted to 50 mL in a three-necked flask, stirring and purging slowly with dry nitrogen at room temperature for 24 h. After that, Na_2TeO_3 (0.01 mol·L^{-1}, 4 mL), mercaptosuccinic acid (50 mg) and $NaBH_4$ (50 mg) were added under vigorous stirring. When the color of the mixture turned to green, the flask was attached to a condenser and refluxed at 100 °C under N_2 flow. The samples were collected at 4 h, 12 h, and 24 h, and washed for three times.

Conjugation of ZnS-CdTe nanospheres to secondary antibody (Ab2)

The conjugation procedure of ZnS-CdTe nanospheres with Ab2 was similar to previous reports [9] by using EDC/NHS as cross reagents. Briefly, 500 μL of the above ZnS-CdTe suspension (2 mg·mL^{-1}) was mixed with 200 μL of Ab2 solution (20 μg·mL^{-1}, in pH 7.4 phosphate buffer). Subsequently, 100 μL of freshly prepared EDC (20 mg·mL^{-1}, in 0.1 M pH 7.4 phosphate buffer) and 100 μL of NHS (10 mg·mL^{-1}, in pH 7.4 phosphate buffer) were added. The samples were incubated 2 h at room temperature under shaking in the dark and kept overnight at 4 °C. The free non-conjugated antibody as well as the isourea byproduct of the conjugation reaction were removed by centrifugation and washed with pH 7.4 phosphate buffer for several times to obtain the Ab2-modified ZnS-CdTe nanospheres(Ab2/ZnS-CdTe). Finally, Ab2/ZnS-CdTe nanospheres were re-dispersed in 500 μL of 1% BSA solution for 2 h, again under stirring, to block the excess carboxyl group and nonspecific binding sites of the ZnS-CdTe/Ab2 nanospheres. After being centrifuged and washed with phosphate buffer, the resultant products were dispersed with 0.05 M of pH 7.4 phosphate buffer to a final volume of 1 mL and stored at 4 °C for later use. The amount of conjugated Ab2 onto the ZnS-CdTe nanospheres was measured by colorimetric bicinchoninic acid (BCA) protein assay as shown in S5 (see supporting information).

The biosensor with dual functionalities for colorimetric and fluorometric determination of AFP

Firstly, the anti-AFP capture antibody (Ab1) was diluted to 4 μg/mL in sodium bicarbonate (100 mM, pH 9.6), and then was added into each well of 96-well PS plate and incubated at 4 °C overnight. The plate was rinsed three times with phosphate buffer and was blocked with 200 μL 1% BSA for 2 h in room temperature to minimize the nonspecific binding. After rinsing five times with phosphate buffer, 100 μL of appropriately diluted AFP solution from 0.0004 ng·mL^{-1}-96 ng·mL^{-1} were added respectively into each well, and the only phosphate buffer was set as the blank. The plate was kept at 37 °C for 1 h and washed with phosphate buffer for five times. Subsequently, 100 μL of Ab2/ZnS-CdTe nanospheres (0.1 mg·mL^{-1}) solution was added into each well and incubated for 40 min at 37 °C. And the plate was rinsed five times with 200 μL of phosphate buffer. And then fluorescence and colorimetry-mode analysis were recorded.

Fluorometric measurement The fluorescence-mode was recorded by a Multiple functional Microwell plates (Spark 10 M, Tecan). The fluorescence spectrum was obtained with

the excitation wavelength of 400 nm and the emission wavelength of 645 nm.

Colorimetric measurement The Triton X-100/sodium dodecyl sulfate (SDS) solution was prepared by dissolving 100 μL of Triton X-100, 90 mg of SDS, 100 μL of anhydrous ethanol and 0.1 g of sodium citrate in 10 mL of the prepared Tris buffer solution. Each well of the above finished bioassay was supplemented with 0.1 mL of 0.1 M HNO_3 solution and mixed thoroughly for 10 min. Then, 3 M NaOH solution was used to adjust the pH of solution to 8.0 and 100 μL of Triton X-100/SDS solution was added to the well and mixed for 3 min. Subsequently, 50 μL of nitro-PAPS solution with 0.1 mmol·L^{-1} was added into each microwell. After mixing for another 8 min, the OD of sample and control blank were measured at 571 nm.

Procedure for HRP-based ELISA

ELISA kit was taken out of the fridge and maintained 30 min before use. And then, 50 μL of target concentrations of analyte (different concentrations of antigens) were added to each microwell. The plate was shaken and then placed in 37 °C for 60 min. After discarding the solution, the plate was washed 5 times with washing buffer to remove the remaining antigen. The plate was incubated with 50 μL HRP-linked antibody for 60 min in 37 °C. Following the same washing steps (5 times), 50 μL chromogenic A and 50 μL chromogenic B were added to the plate successively and then the plate was incubate in 37 °C for 10 min. At last, 50 μL stop solution was added to stop the catalytic process and the OD value of 450 nm was obtained through a microplate reader.

Results and discussion

Characterization of the ZnS-CdTe nanospheres

Our approach relies on the detection antibodies modified by porous ZnS-CdTe nanospheres, which are utilized as the dual mode-detection sensors instead of an enzyme. As shown in Fig. 2a, b and Fig.S1 (ESI), the prepared highly integrated ZnS-CdTe nanospheres are uniformly spherical with a mean diameter of approximately 100 nm. The scanning transmission electron microscopy-high-angle annular dark field (STEM-HAADF) images and EDS-elemental mapping demonstrate that the in-situ fabricated CdTe QDs are successfully embedded into the ZnS nanospheres. The specific surface area of ZnS-CdTe is determined to be about 113 $m^2 \cdot g^{-1}$, a relatively large surface area facilitated to bond plenty of detection antibodies. The average pore diameter of the nanospheres is about 6.2 nm. And the corresponding TEM image of individual CdTe QDs with particle sizes ranging from 6.5 to 8.5 nm is also shown in Fig. 2b and Fig.S1. The incorporated CdTe QDs amounts in the porous ZnS nanospheres can be determined to be 360 QDs per ZnS nanosphere (ESI, Section S3) by inductively coupled plasma atomic emission spectroscopy (ICP-AES). The ZnS-CdTe nanospheres show an excitation peak at 400 nm, and a strong photoluminescence (PL) peak at around 645 nm as shown in Fig. 2d.

Carboxyl functionalized ZnS-CdTe nanospheres were loaded with Ab2 and the amount of conjugated Ab2 was also estimated to be 6600 antibodies per porous ZnS-CdTe nanosphere (see ESI, Section S5), consistent with previous reports [16, 26]. The Ab1 was immobilized on the well in a 96-well plate, and then after repeated washing, the target antigen AFP was bound to Ab1 after blocking with 5% bovine serum albumin (BSA) solution, after another round of washing, the plate was then incubated with the ZnS-CdTe/Ab2 (the bioassay conditions were optimized as shown in ESI, Section 2–6). Washing was once again performed, and then the biomarker can be detected using dual-mode detection of fluorometry and colorimetry.

Dual-mode sensitive assay of disease biomarker based on ZnS-CdTe porous biosensor

Firstly, we investigated a fluorescent bioassay based on the prepared ZnS-CdTe biosensor. QDs has strong and highly stable emission, showing up to 20 times brighter and 100 times more stable against photobleaching than organic dye, rhodamine 6G [27]. Furthermore, herein, the porous structure ZnS nanospheres can enrich plenty of CdTe QDs (loading 360 QDs per porous ZnS nanosphere), which brings about great enhancement of fluorescent bioassay sensitivity. Figure 3a shows the fluorescence spectrum of microplate reader on the wells with an increase of AFP concentration. The fluorescence emission of the target-spotted wells is proportional to the concentration of AFP from 0.04 to 64 ng·mL^{-1} ($r = 0.997$) as shown in Fig. 3b, which shows good quantitative results with the detection limit as low as 0.01 ng·mL^{-1}, defined as blank plus three standard deviations. One control experiment (A) represents the same bioassay that carried out the full approach using Ab2 instead of ZnS-CdTe/Ab2 without adding AFP, while the other control experiment (A0) was also performed on full procedure without addition of target AFP. In each case, the corresponding signal is much smaller than that of the fluorescent bioassay with the lowest concentration of AFP, and the fluorescence of control (A0) is just only a slightly larger than that of control (A) without ZnS-CdTe.

Subsequently, we used the dissolution of porous ZnS nanospheres for signal amplification allowing colorimetry with the bare eye. After incubation of the ZnS-CdTe/Ab2, acid was added to dissolve porous ZnS nanospheres to produce zinc ions. And the dissolution of ZnS nanospheres enables such great amplification that each ZnS nanosphere can generate

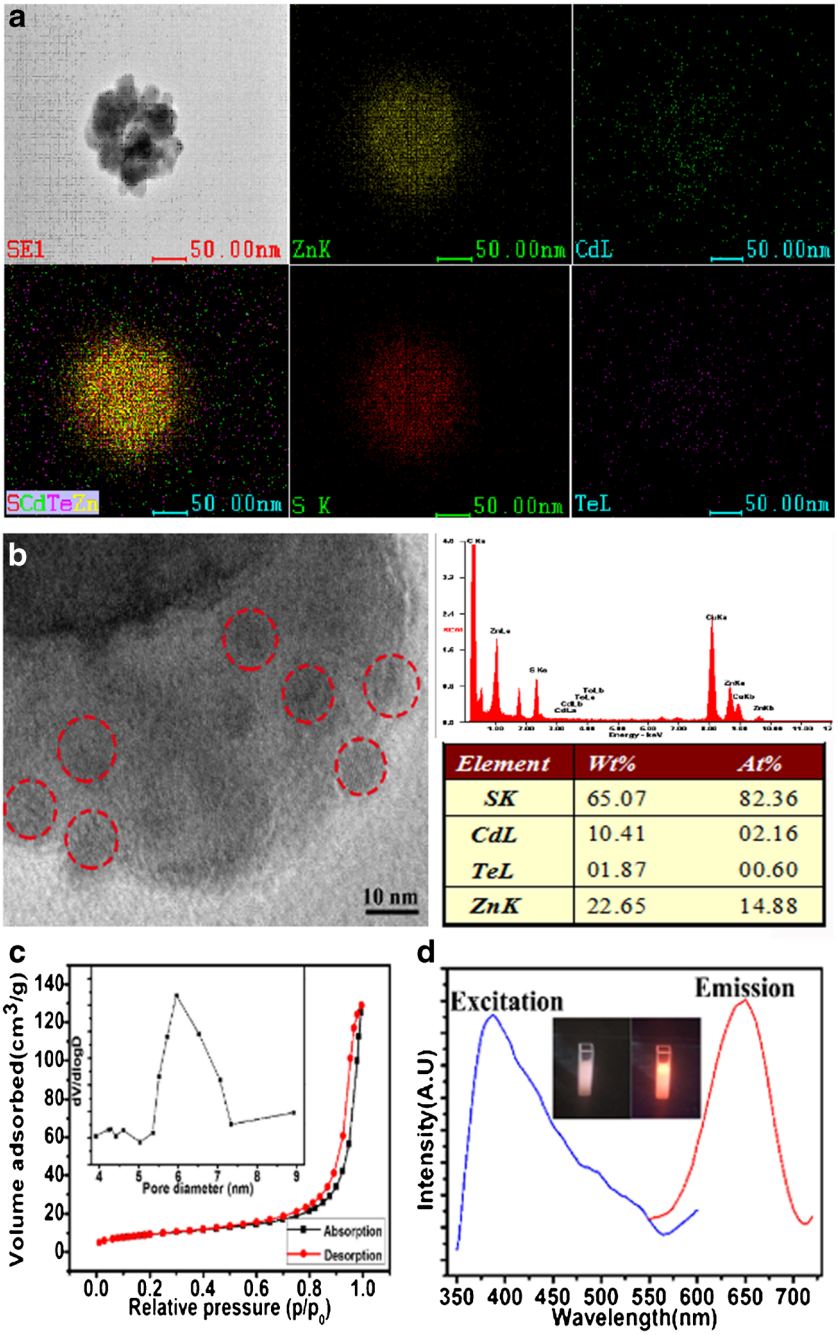

Fig. 2 **a** High-resolution STEM-HAADF images and elemental mapping of ZnS-CdTe nanospheres demonstrate that the in-situ fabricated CdTe QDs are successfully embedded into the ZnS nanospheres. **b** TEM image and EDS-spectral of the ZnS-CdTe nanospheres also indicate the formation of CdTe QDs, and the area of the red circle represents CdTe QDs. **c** N_2 adsorption–desorption isotherms and pore size distribution of the prepared porous ZnS-CdTe nanospheres show porous structure and have a relatively large surface. **d** Excitation and emission spectra of the prepared ZnS-CdTe nanospheres. The inset shows the photographs of the ZnS-CdTe before (left) and after (right) excitation with 365 nm UV light

zinc ions with seven orders of magnitude (ESI, Section S7). Sodium hydroxide was used as a pH adjustor and Nitro-PAPS were added successively to generate the color change from orange to purple in the solution owing to the formation of the zinc complex [28]. UV-Vis spectra of both the pure Nitro-PAPS reagent and the formed zinc complex is shown in Fig. 4. The absorbance at 451 nm, a characteristic absorbance peak for pure Nitro-PAPS, decreased significantly and eventually disappeared within a few minutes (ESI, Section S9, Fig. S6). The maximum absorbance at near 571 nm was occurred owing to the formed zinc complex, while the pure Nitro-PAPS absorption was negligible in this region, thus which can be a blank used in each case. The zinc complex had a maximum absorbance in the pH range 8.0 to 9.0 as shown in Fig. 4b. The dissociation of zinc from protein-bound zinc at pH 8.0 buffer was also examined as shown in Fig. S5, and almost 100% of the protein-bound zinc was successfully dissociated by using Triton X-100/SDS solution which usually served as protein-bound metal ion dissociation reagent [28]. Addition quantum of Nitro-PAPS reagent was also optimized to be 0.1 mM for the next experiments (ESI, Section 10).

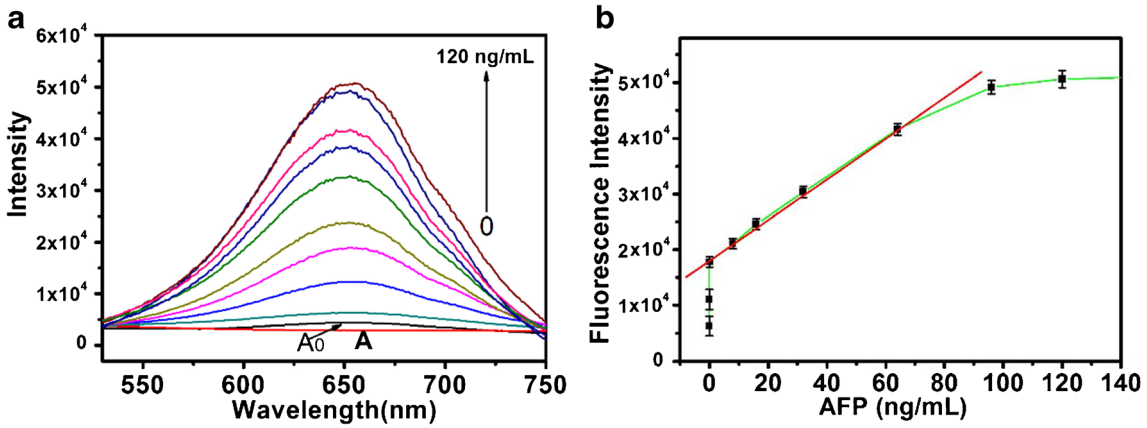

Fig. 3 **a** Fluorescent spectrum of each microwell with different AFP concentrations at 400 nm excitation by a UV/Vis/FL microplate reader. **b** Response plot of the fluorescence signals (F) versus different concentrations of AFP with emission of 645 nm at 400 nm excitation. Error bars indicate one standard deviation from the mean of three assays

Figure 5 shows that the solution exhibited purple only in the presence of AFP, and deeper purple was generated with a higher concentration of AFP. Control experiment performed by spiking an unrelated bovine serum albumin (BSA) resulted in no color change. For the demonstration of the effect on the normal serum Zn or increased serum Zn concentrations due to hemolysis, lipemia and icterus, the other control experiment by addition a series of Zn into BSA as samples also indicated no instinct interference with the assay in Fig. 5b. The optical density (OD) value increased with the AFP concentration, and a linear relationship ($r = 0.998$) between OD value and AFP concentration in the range of 0.05–12 ng·mL^{-1} was observed. And the limit of detection defined as a signal three times higher than the standard deviation of the blank is 0.007 ng·mL^{-1}.

Comparison of dual-mode bioassay with other bioassays

Conventional horseradish peroxidase (HRP)-based ELISA as a standard protocol was compared with our bioassay (ESI, Section S11). As shown in Fig. S8, an AFP concentration as low as 0.005 ng·mL^{-1} can be detected by the distinct color difference in solution (even can be discriminated through bare-eyes) using our colorimetry approach, whereas it needed nearly a concentration of 1.5 ng·mL^{-1} for colorimetric differentiation in conventional ELISA. The results indicate an at least 1000-fold decrease in the limit of detection compared with the ELISA. The sensitivity and linear range of our bioassay was also compared with those of other methods in the latest published reports for disease biomarker determination as shown in Table 1. Obviously, both of the colorimetric detection and fluorescent modes possessed higher sensitivity than that of the previous detection, and which high sensitivity was achieved by the unique two-round signal amplification.

Besides, the important enzymatic process as biological signal amplification in the ELISA needs well-defined conditions, and the optical density (OD) value is not always stable in a certain period, for instance, that should be determined within 15 min otherwise the OD would decrease [2]. On the contrary, in our bioassay, no distinct change in fluorescence and colorimetry signal was observed within 120 min after an immunoreaction as shown in Fig. S9, indicating the signal

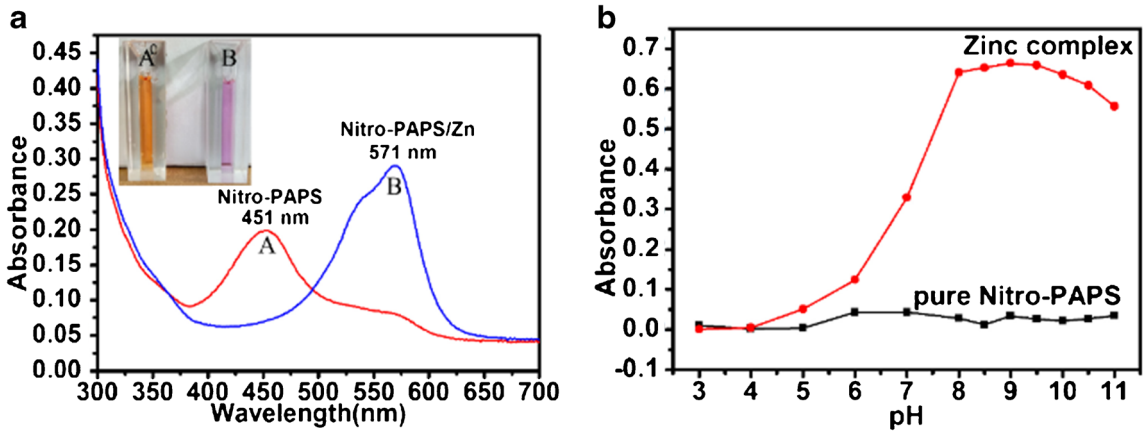

Fig. 4 **a** Absorbance curves for pure 0.05 mM Nitro-PAPS reagent solutions and further formed Zinc Complex (Nitro-PAPS/Zn, 0.5 mg·L^{-1} of Zn^{2+}). Inset is the corresponding photo image with the solutions. **b** Effect of pH on pure Nitro-PAPS and Zinc Complex (Nitro-PAPS/Zn)

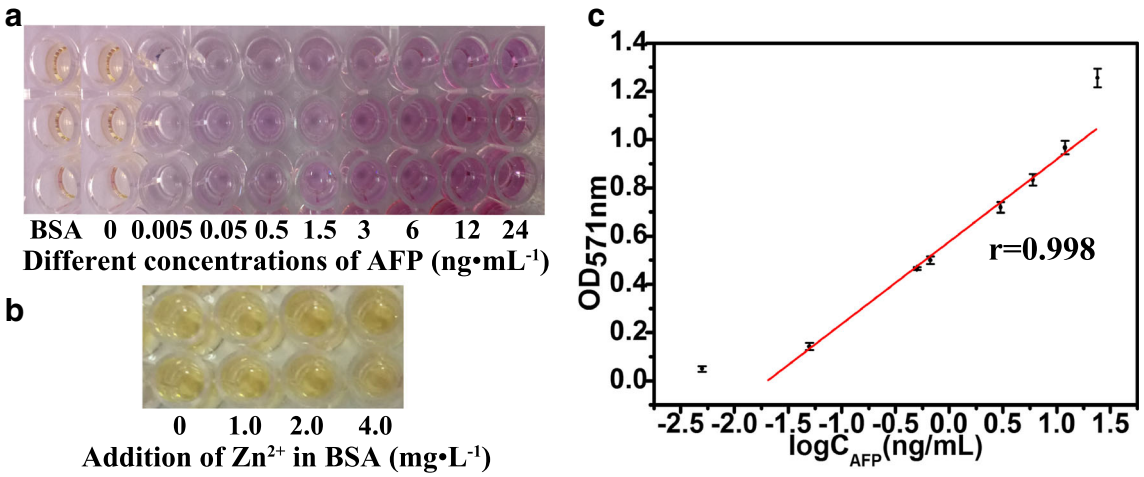

Fig. 5 **a** Photograph showing the performance of AFP colorimetry detection using ZnS-CdTe nanospheres as labels. **b**. Photography showing the no instinct interference with the assay by adding different concentrations of Zn^{2+} into BSA. **c** The response plot of the OD value with 571 nm versus different concentrations of AFP. An error bar indicates one standard deviation from the mean of three assays

amplification through robust chemical reaction is stable and advantaged for practical application. Long-term storage stability was also further investigated by comparison of the slopes from the corresponding calibration plots. As shown in Fig.S10, the values of slopes obtained by fluorometry and colorimetry assay have no obvious change after 30-day storage at 4 °C, indicated that a porous ZnS-CdTe nanosensors is very efficient for retaining the bioactivity and preventing the biomolecules from leaking out because of the strong covalent linkage between ZnS-CdTe nanospheres and mercapto or primary amine groups in these biomolecules.

The utility of the bioassay was also investigated by analyzing three serum samples, in comparison with the ELISA method. Table S1 describes the correlation between the results by our bioassays as well as the ELISA method. The relative deviations of fluorometry and colorimetry bioassay compared with ELISA assay were respectively in the range of −4.3 to 9.4%, indicating no significant difference. The results also showed that the recoveries were in the range of 94%–109%, and the relative standard deviation (RSDs) were in the range of 1.7%–3.6%. Although the dual-mode assays will need more complex optical instrumentation than typical ELISA colorimetric assays, they can indeed be a suitable alternative to ELISA in clinical diagnostic and can be further potentially utilized as a commercial kit since the ZnS-CdTe nanoparticles as biosensors can be easily obtained at a low cost.

Conclusion

We are introducing an enzyme-free bioassay for robust dual-mode sensitive detection by fluorometry and colorimetry for disease biomarkers in serum based on porous ZnS-CdTe biosensor. Sensitive fluorometry detection can be achieved directly by an increase of the ZnS-CdTe loading per sandwich immunoreaction, and the zinc-based amplification strategy is

Table 1 Comparison of the dual-mode bioassay system with other latest methods for disease marker detection

Detection technique	Linear range(ng·mL^{-1})	Detection limit(ng·mL^{-1})	References
Fluorescent molecularly-imprinted polymer	3.96–80.0	0.42	[29]
Fluorescent immunosensor	0.1–5.0	0.012	[30]
Enhanced immunofluorescence	0.1–10	0.07	[2]
Fluorescent QDs	6–100	0.062	[31]
Quantum Dots Nanobeads	0.133–2.5 ng	0.133 ng	[17]
Fluorescent detection of this work	0.04–64	0.01	
ELISA-like system based nanobody	0.1–1000	0.48	[32]
Colorimetric Immunoassay	–	0.1	[3]
Upconversion nanoparticle as elemental tag	0.5–35	0.31	[33]
Chemiluminescence enzyme-linked immunosorbent	2–500	0.02	[34]
Colorimetric detection of this work	0.05–12	0.007	

efficient and robust thanks to the chemical dissolution of ZnS nanospheres into millions of zinc ions, which can directly develop a colorimetric bioassay by using Nitro-PAPS to form purple complex. We believed that the biosensor can also potentially be adapted for the detection of other biomarkers, proteins and DNA.

Acknowledgments We sincerely appreciate the National Natural Science Foundation of China for the financial support (81573388). This work was supported by "Qing Lan Project of Jiangsu province" and "Six talent peaks project of Jiangsu Province (YY-032)". This work was also supported by the Open Project Program of Jiangsu Key Laboratory for Pharmacology and Safety Evaluation of Chinese Materia Medica (No. JKLPSE201805) and the Project of the Priority Academic Program Development of Jiangsu Higher Education Institutions (PAPD).

Compliance with ethical standards The author(s) declare that they have no competing interests.

References

1. Patton JC, Coovadia AH, Meyers TM, Sherman GG (2008) Evaluation of the ultrasensitive human immunodeficiency virus type 1 (HIV-1) p24 antigen assay performed on dried blood spots for diagnosis of HIV-1 infection in infants. Clin Vaccine Immunol 15:388–391
2. Zhao LJ, Yu RJ, Ma W, Han HX, Tian H, Qian RC, Long YT (2017) Sensitive detection of protein biomarkers using silver nanoparticles enhanced immunofluorescence assay. Theranostics 7:876–883
3. Zhu GB, Lee HJ (2017) Electrochemical sandwich-type biosensors for α-1 antitrypsin with carbon nanotubes and alkaline phosphatase labeled antibody-silver nanoparticles. Biosens Bioelectron 89:959–963
4. Cui C, Chen Y, Jiang DC, Zhu JJ, Chen HY (2017) Attomole antigen detection using self-Electrochemiluminous graphene oxide-capped au@L012 nanocomposite. Anal Chem 89:2418–2423
5. Xu SX, Li XM, Li CB, Li JL, Zhang XF, Peng W, Hou XD (2016) In situ generation and consumption of H2O2 by Bienzyme-quantum dots bioconjugates for improved Chemiluminescence resonance energy transfer. Anal Chem 88:6418–6424
6. Cao J, Wang W, Bo B, Mao X, Wang K, Zhu X (2017) A dual-signal strategy for the solid detection of both small molecules and proteins based on magnetic separation and highly fluorescent copper nanoclusters. Biosens Bioelectron 90:534–541
7. Lin H, Liu Y, Huo J, Zhang A, Pan Y, Bai H, Jiao Z, Fang T, Wang X, Cai Y, Wang Q, Zhang Y, Qian X (2013) Modified enzyme-linked immunosorbent assay strategy using graphene oxide sheets and gold nanoparticles functionalized with different antibody types. Anal Chem 85:6228–6232
8. He J, Liu Y, Babu T, Wei Z, Nie Z (2012) Self-assembly of inorganic nanoparticle vesicles and tubules driven by tethered linear block copolymers. J Am Chem Soc 134:11342–11345
9. De IR, Stevens MM (2012) Plasmonic ELISA for the ultrasensitive detection of disease biomarkers with the naked eye. Nat Nanotechnol 7:821–824
10. Zou ZX, Du D, Wang J, Smith JN, Timchalk C, Li YQ, Lin YH (2010) Quantum dot-based immunochromatographic fluorescent biosensor for biomonitoring trichloropyridinol, a biomarker of exposure to chlorpyrifos. Anal Chem 82:5125–5133
11. Liu DB, Wang ZT, Jin A, Huang XL, Sun XL, Wang F, Yan Q, Ge SX, Xia NS, Niu G, Liu G, Hight Walker AR, Chen XY (2013) Acetylcholinesterase-catalyzed hydrolysis allows ultrasensitive detection of pathogens with the naked eye. Angew Chem Int Ed 52: 14065–14069
12. Qu W, Liu Y, Liu D, Wang Z, Jiang X (2011) Copper-mediated amplification allows readout of immunoassays by the naked eye. Angew Chem Int Ed 50:3442–3445
13. Ye HH, Yang KK, Tao J, Liu YJ, Zhang Q, Habibi S, Nie ZH, Xia XH (2017) An enzyme-free signal amplification technique for ultrasensitive colorimetric assay of disease biomarkers. ACS Nano 11:2052–2059
14. Li JX, Gao ZQ, Ye HH, Wan SL, Pierce MH, Tang DP, Xia XH (2017) A non-enzyme cascade amplification strategy for colorimetric assay of disease biomarkers. Chem Commun 53:9055–9058
15. Dong H, Yan F, Ji H, Wong DK, Ju HX (2010) Quantum-dot-functionalized poly(styrene-co-acrylic acid) microbeads: step-wise self-assembly, characterization, and applications for sub-femtomolar electrochemical detection of DNA hybridization. Adv Funct Mater 20:1173–1179
16. Xiang Y, Zhang HX, Jiang BY, Chai YR, Yuan R (2011) Quantum dot layer-by-layer assemblies as signal amplification labels for ultrasensitive electronic detection of uropathogens. Anal Chem 83: 4302–4306
17. Zhang LN, Deng HH, Lin FL, Xu XW, Weng SH, Liu AL, Lin XH, Xia XH, Chen W (2014) In situ growth of porous platinum nanoparticles on graphene oxide for colorimetric detection of cancer cells. Anal Chem 86(5):2711–2718
18. Qian J, Dai HC, Pan XH, Liu SQ (2011) Simultaneous detection of dual proteins using quantum dots coated silica nanoparticles as labels. Biosens Bioelectron 28:314–319
19. Li J, Zhao XW, Zhao YJ, Gu ZZ (2009) Quantum-dot-coated encoded silica colloidal crystals beads for multiplex coding. Chem Commun (17):2329–2331
20. Tan L, Chen K, Huang C, Peng R, Luo X, Yang R, Cheng Y, Tang Y (2015) A fluorescent turn-on detection scheme for α-fetoprotein using quantum dots placed in a boronate-modified molecularly imprinted polymer with high affinity for glycoproteins. Microchim Acta 182:2615–2622
21. Hierlemann A, Gutierrez-Osuna R (2008) Higher-order chemical sensing. Chem Rev 108:563–613
22. Wu P, Miao LN, Wang HF, Shao XG, Yan XP (2011) A multidimensional sensing device for the discrimination of proteins based on manganese-doped ZnS quantum dots. Angew Chem Int Ed 50: 8118–8121
23. Gutierrez-Osuna R, Hierlemann A (2010) Adaptive microsensor systems. Annu Rev Anal Chem 3:255–276
24. Jin C, Kurzawski P, Hierlemann A, Zellers ET (2008) Evaluation of multitransducer arrays for the determination of organic vapor mixtures. Anal Chem 80:227–236
25. Kim KK, Hong S, Cho HM, Lee J, Suh YD, Ham J, Ko SH (2015) Highly sensitive and stretchable multidimensional strain sensor with Prestrained anisotropic metal nanowire percolation networks. Nano letter 15:5240–5247
26. Krishnan S, Mani V, Wasalathanthri DP, Kumar CV, Rusling JF (2011) Attomolar detection of a Cancer biomarker protein in serum by surface Plasmon resonance using superparamagnetic particle labels. Angew Chem 123:1207–1210
27. Chan WCW, Nie SM (1998) Quantum dot bioconjugates for ultrasensitive nonisotopic detection. Science 281:2016–2018
28. Makino T, Kiyonaga M, Kina K (1988) A sensitive, direct colorimetric assay of serum iron using the chromogen, nitro-PAPS. Clin Chim Acta 171:19–28

29. Karfa P, Roy E, Patra S, Kumar D, Madhuri R, Sharma PK (2016) A fluorescent molecularly-imprinted polymer gate with temperature and pH as inputs for detection of alpha-fetoprotein. Biosens Bioelectron 78:454–463
30. Xie QF, Weng XH, Lu LJ, Lin ZY, Xu XW, Fu CL (2016) A sensitive fluorescent sensor for quantification of alpha-fetoprotein based on immunosorbent assay and click chemistry. Biosens Bioelectron 77:46–50
31. Morales-Narvaez E, Monton H, Fomicheva A, Merkoci A (2012) Signal enhancement in antibody microarrays using quantum dots nanocrystals: application to potential Alzheimer's disease biomarker screening. Anal Chem 84: 6821–6827
32. Chen J, He QH, Xu Y, Fu JH, Li YP, Tu Z, Wang D, Shu M, Qiu YL, Yang HW, Liu YY (2016) Nanobody medicated immunoassay for ultrasensitive detection of cancer biomarker alpha-fetoprotein. Talanta 147:523–530
33. Liu ZR, Yang B, Chen BB, He M, Hu B (2016) Upconversion nanoparticle as elemental tag for the determination of alpha-fetoprotein in human serum by inductively coupled plasma mass spectrometry. Analyst 142:197–205
34. Maiolini E, Ferri E, Pitasi AL, Montoya A, Giovanni MD, Erranic E, Girotti S (2014) Bisphenol a determination in baby bottles by chemiluminescence enzyme-linked immunosorbent assay, lateral flow immunoassay and liquid chromatography tandem mass spectrometry. Analyst 139:318–324